

RESTRAINED SHRINKAGE - ITS IMPACT ON THE RESPONSE OF REINFORCED CONCRETE MEMBERS

T. S. Ahn, and V. S. Gopalaratnam,
Department of Civil Engineering, University of Missouri-Columbia
Columbia, Missouri 65211, U.S.A.

Abstract

The test set-up developed during this investigation allowed the monitoring deformations from three hour onwards on a large reinforced tension specimen. Companion unreinforced specimen of the same size, exposed to same conditions of curing and drying served as the reference unrestrained sample. Three one-inch diameter deformed steel bars were used to provide internal restraint to the membrane specimen. Given the relatively small cross-sectional dimensions compared to the length, the specimen geometry lent itself well to a one-dimensional analysis of stress transfer between the concrete matrix and steel reinforcing bars. Residual tensile stress in the concrete of approximately 40% of the tensile strength was computed from the model. Since drying shrinkage is a size and geometry dependent phenomenon, residual stresses due to restrained shrinkage are expected to contribute additionally to the size and geometry effects attributed to brittle fracture in reinforced concrete members.

1 Residual stress due to restrained shrinkage

Drying shrinkage results in volumetric changes in concrete. Since the rate of drying is typically different for the exterior surfaces compared to the interior of a concrete member, differential volumetric changes take place. Residual stresses due to drying shrinkage are of a self-equilibrating nature. As a result, the interior of concrete members undergoing drying are typically subjected to compressive stresses while the exterior surfaces are subjected to tensile stresses (Wittmann, 1982). In some instances these stresses may be locally high enough to cause shrinkage cracking. However, if one characteristic dimension of the member is significantly larger than the other two, the drying process can essentially be assumed to be one-dimensional in nature. This simplification is analytically attractive in a reinforced concrete specimen because it is then logical to neglect the residual stress distributions due to transverse differential drying of plain concrete compared to the residual stress resulting from the restraint provided by the reinforcing steel. In general however, the drying process and the restraint provided by the reinforcing steel are both three dimensional processes that may cause measurable variations in strains across the transverse directions of the reinforced concrete member. The present investigation adopts a one-dimensional approach for modeling the first-order effects due to restrained shrinkage.

1.1 Bilinear model

Consider the idealized specimen shown in schematic form in Fig. 1(a). The restraint provided by the steel reinforcement typically develops gradually from the specimen ends. For a sufficiently long specimen, a bilinear steel strain distribution is expected. For shorter specimens linear or parabolic distributions are likely (Ahn, 1995). The bilinear steel strain distribution is assumed as

$$\varepsilon_s^\sigma(x) = \varepsilon_{s\max}, \quad 0 \leq x \leq \frac{L - L_t}{2} \quad (1)$$

$$\varepsilon_s^\sigma(x) = \varepsilon_{s\max} \left[1 - \frac{2\left(x - \frac{L}{2} + \frac{L_t}{2}\right)}{L_t} \right], \quad \frac{L - L_t}{2} \leq x \leq \frac{L}{2}$$

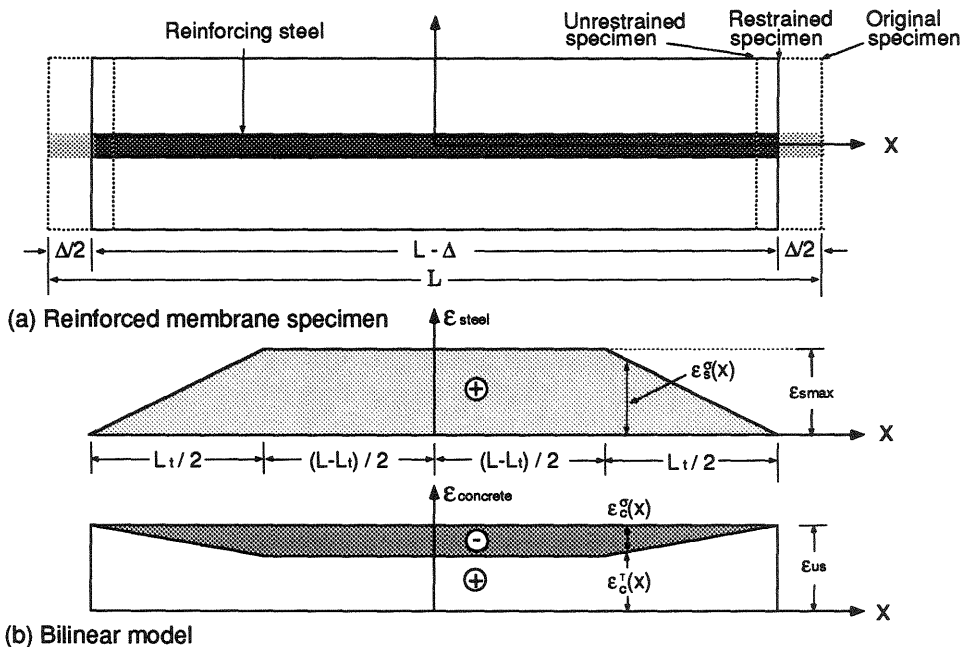


Fig. 1. One-dimensional models for computation of residual stresses due to restrained shrinkage in reinforced tension membranes

where $\epsilon_{s\max}$ is the maximum steel strain, L and L_t are the original length of the reinforced membrane specimen and transition length, Fig. 1, respectively. The transition length is assumed to be governed by the same mechanism used for development length, l_d , in the design of reinforced concrete, and hence the same rate of strain development is assumed, ie.

$$L_t = \frac{\epsilon_{s\max}}{\epsilon_y} l_d \quad (2)$$

Since the restrained shrinkage stresses are self-equilibrated, the residual strain in concrete is given by

$$\epsilon_c^\sigma(x) = -\epsilon_s^\sigma(x) \frac{E_s A_s}{E_c A_c} \quad (3)$$

The total strain in the concrete constituent of the reinforced membrane specimen can be expressed as

$$\varepsilon_c^T(x) = \varepsilon_{us} + \varepsilon_c^\sigma(x) \quad (4)$$

where ε_{us} is the uniform average strain along the length of an unrestrained concrete specimen, $\varepsilon_c^\sigma(x)$ is the strain due to residual shrinkage stress resulting from the self-equilibrating condition, and $\varepsilon_c^T(x)$ is the resultant strain distribution for the concrete constituent of a reinforced concrete specimen. Superposition is valid due to the elastic nature of the macroscopic response in this case.

Total deformation in steel, Δ_s , and concrete, Δ_c , can be calculated by integrating the respective strain distributions along the length of the specimen as

$$\Delta_s = 2 \left[\int_0^{L/2} \varepsilon_s^\sigma(x) dx \right] = \varepsilon_{s\max} \left(L - \frac{L_t}{2} \right) \quad (5)$$

$$\Delta_c = 2 \left[\int_0^{L/2} \varepsilon_c^T(x) dx \right] = \varepsilon_{us} L - \varepsilon_{s\max} \left(L - \frac{L_t}{2} \right) \frac{E_s A_s}{E_c A_c} \quad (6)$$

$\varepsilon_{s\max}$ can be determined by compatibility condition, $\Delta_s = \Delta_c = \Delta$ as follow

$$\varepsilon_{s\max} = \varepsilon_{us} \left(\frac{E_c A_c}{E_c A_c + E_s A_s} \right) \left(\frac{L}{L - \frac{L_t}{2}} \right) \quad (7)$$

In many practical problems it is often of interest to be able to predict the maximum residual stress in steel and concrete constituents of a reinforced concrete member, given the basic material properties of the constituents and the geometric details of the composite member. Given the concrete type and member characteristics it is possible to compute the unrestrained shrinkage strain in concrete using empirical formulae recommended in model codes (ACI, 1992 and Bazant, 1982). Alternately, as in the current investigation, this has been measured from actual drying tests. The maximum steel strain can be determined, using compatibility of steel and concrete deformations, by solving the quadratic equation.

$$\frac{l_d}{2\varepsilon_y} \frac{E_c A_c + E_s A_s}{E_c A_c} \varepsilon_{s\max}^2 - L \frac{E_c A_c + E_s A_s}{E_c A_c} \varepsilon_{s\max} + \Delta_u = 0 \quad (8)$$

where Δ_u is the unrestrained shrinkage deformation in concrete.

Deformation of the restrained member can then be predicted using Eqs. 5 and 6. The maximum tensile strain in concrete is given by Eq. 3, where $\epsilon_s^\sigma(x)$ is replaced by ϵ_{smax} . Maximum residual stress in concrete is then obtained assuming elastic behavior.

It should be noted that the bilinear model can be effectively used to study the range of restrained tensile stress in concrete by varying the transition length in the limit $0 \leq L_t \leq L$. $L_t = 0$ represents one extreme case where the strain distribution is assumed uniform along the entire length of the specimen. $L_t = L$ represents the other extreme where linear variation of strain from a zero value at the ends to a maximum value ϵ_{smax} at the crack of the specimen.

Actual local strain distribution measurements in the reinforcing bar and/or the concrete matrix though useful, requires a lot of effort if accuracy and reliability of long-term data is desired. Several alternate and rationally plausible strain distributions can be analytically studied. The linear model (which is a special case of the bilinear model as stated earlier) and parabolic model which are perhaps suitable for shorter specimens are of interest. These models are simpler because these do not include the transition length parameter. Details of these models are included in Ahn (1995). For the same overall deformation, the bilinear model predicts the lowest residual tensile stress in concrete. The highest values are predicted by the linear model. The parabolic model predicts residual stress values between the linear and bilinear models.

2 Experimental program

The restrained shrinkage test program was developed to provide support information about residual stress for a larger study on tensile stiffening in reinforced concrete tension membranes. Two normal strength specimens with dimensions identical to that used for the tension membranes (ρ , the steel to composite area ratio of 3.27%) were cast for the purpose of making shrinkage measurements. One of these was an unreinforced specimen to provide data on unrestrained shrinkage deformations. The other was a specimen that had longitudinal reinforcement identical to the tension membranes (no lateral reinforcement). This specimen allowed deformation measurements due to restrained shrinkage both on the concrete and steel constituents.

Both specimens were cast indoors in specially designed forms, that allowed deformation measurements from as early as three hours after casting, Fig. 2. The specimens were cast with its 50" x 12" (127 x 30.5 cm) face exposed. This face has been designated as "top face" in all subsequent reference. The top face was covered with plastic sheet to minimize moisture loss during the first hour after casting. Thereafter this face was covered with wet burlap and plastic sheet. Deformation measurements on this top face were made from 3 hours up to 5 days on a prescribed schedule that was determined based on the expected deformations. These measurements during the "setting period" were made with the formwork still in place. Measurements from three dial gages (one for deformation in the unrestrained specimen and one each for concrete and steel deformations in the restrained specimen) were made on 3-hourly intervals for the first day, 6-hourly intervals for the second day, 12 hourly intervals for the third day, and once a day for the last two days. Concrete deformations were made using a gage length of 44" (112 cm), while steel deformations were measured using a 56" (142 cm) gage length. The resolution of the deformation measurements (0.0025 mm) and the length of

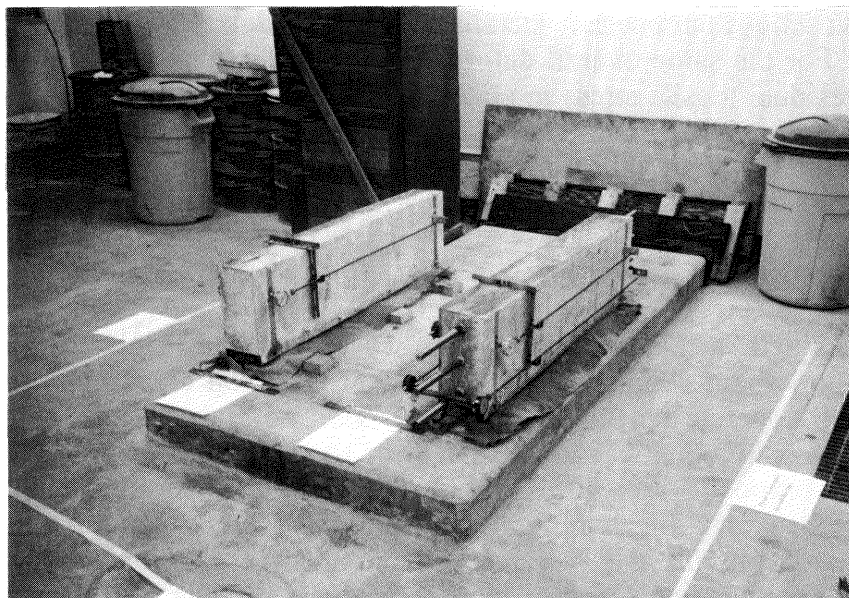


Fig. 2. Overall view of the set-up used for shrinkage measurements during the drying period (29 days ~ 120 days)

the specimen facilitated reliable shrinkage strain measurements including initial expansion due to heat from the hydration process.

At an age of 5 days after casting, the specimen was demolded and turned on its side, 50" x 6" (127 cm x 15 cm) face, so that measurements from this time onwards could be made both on the top and bottom faces. Minimal movement of the specimen during demolding and turning it on the side allowed continuity of deformation measurements on the top face (from the "setting" to the "curing" periods). The specimen during this "curing period" (6-28 days) was completely wrapped in wet burlap and plastic, with only the dial gages exposed for monitoring shrinkage deformations. A plastic sheet on the face contacting the floor ensured that restraint due to friction was minimized. Six dial gages were monitored (same set of dial gages affixed for the bottom face, as described earlier for the top face) once a day during this curing period.

The plastic sheet and wet burlap were removed after 28 days, subjecting the specimens to drying under normal laboratory conditions (approximately 73°F, 26% R.H.). Deformation measurements during this "drying period" were carried out once a day until 100 days and once a week thereafter until 180 days. The shrinkage test was terminated after 180 days when it was observed that deformations due to shrinkage beyond 120 days were very small and of magnitude comparable to deformations from temperature variations in the laboratory.

3 Results and discussions

Results from the unrestrained and restrained shrinkage tests are summarized in Fig. 3. Open symbols represent measurements made on the top face of the specimen. Filled symbols represent measurements made on the bottom face of the specimen. Triangular symbols in Fig. 3 are used for the results from the unrestrained shrinkage test on plain concrete specimen. Square symbols represent measurements made on the concrete constituent and circular symbols represent measurements made on the steel constituent of the restrained shrinkage reinforced concrete specimen. Fig. 3 presents results from three distinct stages of the shrinkage test. The first stage includes the initial setting stage which also exhibits thermal expansion resultant from the heat of hydration and is identified in the enlarged inset as "setting period". The first measurements were made starting as early as 3 hours after the casting. This stage lasted for 120 hrs (5 days) after casting. The second stage covered the curing period until the end of which

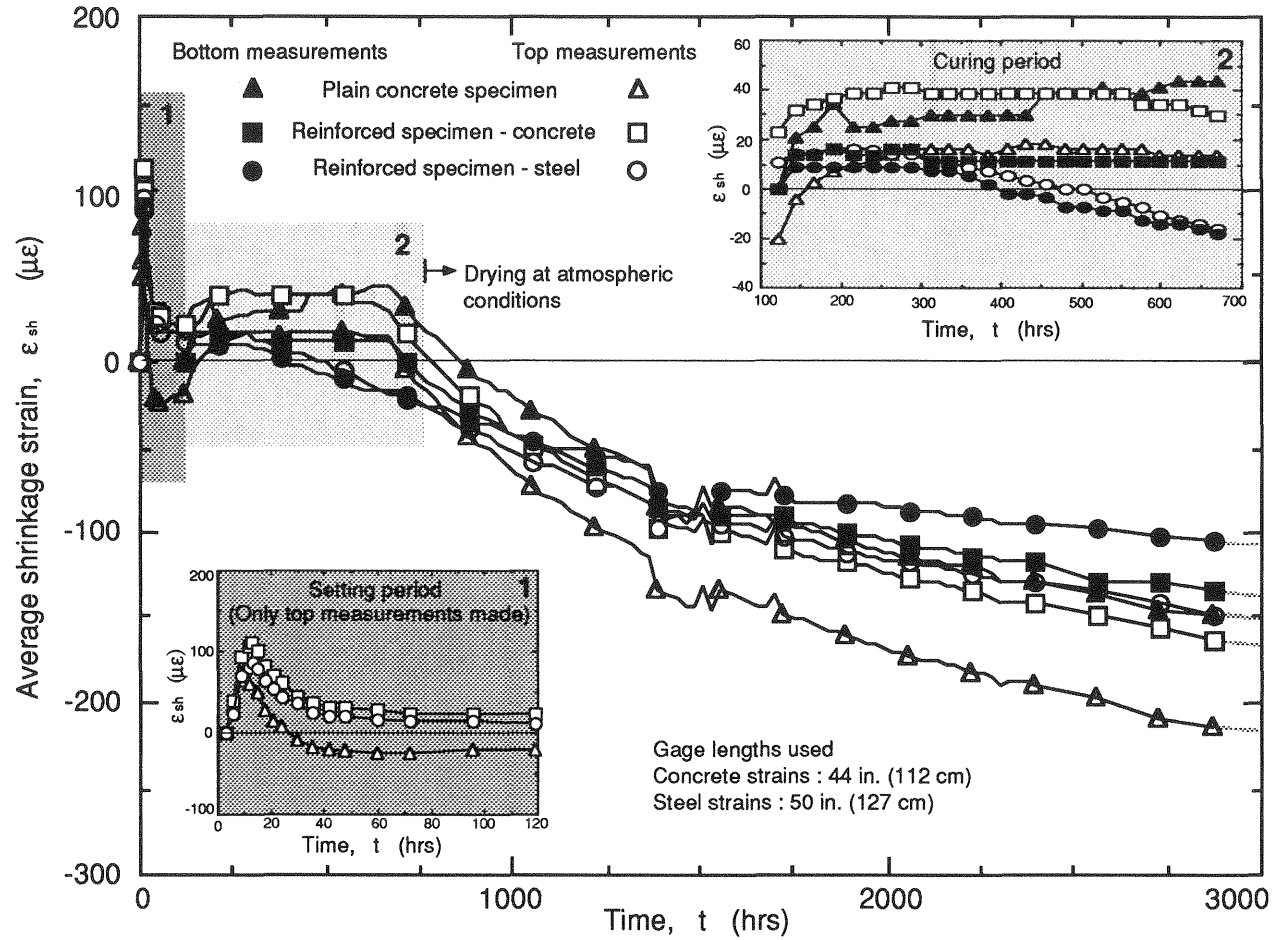


Fig. 3. Specimen deformation during initial setting, curing and drying periods

no significant moisture migration took place. This stage has been identified in the enlarged inset as "curing period" (6-28 days). The third stage is the drying stage which accounts for much of the deformations of interest as far as this investigation is concerned. These deformations also have a great deal of importance as far as practical analysis and design are concerned. Shrinkage measurements have been reported from when drying begins (29 days) up to approximately 2,900 hrs (120 days) after casting. The rate of shrinkage becomes smaller with time and changes in deformation beyond 120 days for these specimens are relatively small.

Since the test set-up was specifically designed to make accurate early age measurements, it was possible to record thermal expansion in both the steel and concrete constituents for the first 12 hours. Given the practical constraints, only top face shrinkage measurements was possible during this stage (see inset 1). Peak values of tensile strains measured during the first stage in the steel and concrete constituents of the restrained shrinkage specimen were in the $100 \mu\epsilon$ range which corresponds to an approximate average temperature increase of $17^\circ F$.

Just like in the first stage, the specimens were kept wrapped in plastic to prevent moisture migration and resultant drying. The relative humidity within the wrapped enclosure was in the 98-100% range. All deformations during this period were expected to be near zero. However strain values in the range $-20 \mu\epsilon$ (shrinkage or compressive) to $40 \mu\epsilon$ (expansion or tensile strain) were recorded (see inset 2). The initial expansion observed in Inset 2 of Fig. 3 is due to swelling associated with the rewetting of burlap covering the specimens at the start of the curing stage. While the concrete deformations show no significant changes in the curing period, the steel reinforcing bars appear to exhibit small amounts of shortening ($\text{approximately } 30 \mu\epsilon$). Even though these strains are small in comparison to the shrinkage strains measured at 120 days, the reasons for the shortening in steel without comparable shortening in concrete is not clear.

The third stage is the drying stage which accounts for much of the deformations of interest as far as this investigation is concerned. Results from the shrinkage measurements during the drying period (29-120 days) are summarized in Table 1 independently for the top and bottom faces. It should be noted that "top" and "bottom" are references to the original casting configuration. During the drying period, both the "top" and "bottom" faces were in fact vertical and subjected to comparable conditions of drying. Values reported for deformations measured on the top face are typically larger than those reported for the bottom face. This is attributed to the fact that the top face is water-rich compared to the bottom face, and

Table 1. Comparison of experimentally measured restrained shrinkage deformation with analytical predictions using the bilinear restrained shrinkage model

Experimental values		Analytical predictions			Difference $\frac{(\Delta_{rs})_a - (\Delta_{rs})_e}{(\Delta_{rs})_a + (\Delta_{rs})_e} \cdot 2$ (%)
Average unrestrained shrinkage strain ϵ_{us} ($\mu\epsilon$)	Restrained shrinkage deformation $(\Delta_{rs})_e$ (μin)	Maximum steel strain (compressive) ϵ_{smax} ($\mu\epsilon$)	Transition length L_t (in.)	Restrained shrinkage deformation $(\Delta_{rs})_a$ (μin)	
193 Bottom	7300 (0.185 mm)	163	3.89 (9.88 cm)	7800 (0.198 mm)	6.6
	4300 (0.109 mm)				57.9
227 Top	9700 (0.246 mm)	193	4.60 (11.68 cm)	9200 (0.234 mm)	-5.3
	6500 (0.165 mm)				34.4

consequently is subjected to more local volumetric changes due to moisture migration.

Experimentally measured restrained shrinkage deformations are compared in Table 1 with deformations predicted analytically using the one-dimensional bilinear model of the restrained shrinkage specimen developed earlier. The model requires unrestrained shrinkage strain in concrete, elastic modulus of steel and concrete, steel and concrete cross-sectional areas, and specimen length as input parameters. Model predicted ϵ_{smax} values for the top and bottom face measurements are 193 and 163 $\mu\epsilon$ respectively. The corresponding values of the transition length, L_t , are 4.60 (11.68 cm) and 3.89 in (9.88 cm). The small transition length, (compared to the specimen length) values indicate that the average strain distribution very nearly equals the maximum strain values in both the steel and concrete constituents. Predicted restrained shrinkage deformations compare very well with those measured in the concrete constituent of the reinforced concrete specimen - 7,800 μin (0.198 mm) and 9,200 μin (0.234 mm) predicted for the top and bottom faces respectively compared to corresponding experimental values of 7,300 μin (0.185 mm) and 9,700 μin (0.246 mm) respectively. This corresponds to errors of 6.6% and -5.3% for the top and bottom face measurements, respectively. The experimental

deformations measured in the reinforcing steel are however significantly smaller. This can be attributed to a combination of two effects: (1) the restraint provided by the steel becomes less effective as the transverse distance from the steel reinforcement becomes larger, and (2) unrestrained shrinkage is smaller in the interior where less drying occurs compared to the exterior surfaces. These second-order influences resultant from the transverse variations in unrestrained shrinkage and the mechanics of the restraint imposed in the transverse directions can only be modelled using a comprehensive 3-dimensional treatment of the restrained shrinkage problem.

Given the observation that the model predictions of the overall restrained shrinkage deformation are acceptable for first-order analysis of residual shrinkage stress in reinforced concrete, two extremes in strain distribution are possible: (1) steel strain is uniform along the length of the specimen, and (2) steel strain develops from zero at the ends to a maximum value at the center of the specimen. As far as the bilinear model is concerned, the first case is approached when the transition length $L_t \rightarrow 0$. The second case is approached when the transition length $L_t \rightarrow L$ (also equivalent to the linear model). The maximum residual stresses in steel and concrete in the first case are lower bound estimates of the actual stresses, while they are the upper bound estimates in the second case. Given the small values estimated for the transition length, Table 1, the bilinear model predictions of the maximum tensile stress in concrete can be assumed to conservative. Even the most conservative estimate suggests that the maximum residual stress in concrete is in the range of 35~40% of the concrete tensile strength.

4 Influence of residual stress due to restrained shrinkage on tensile stiffening response

As described earlier this study was initiated in support of a larger investigation dealing with the tensile stiffening effect of concrete in reinforced tension membranes after it was speculated that differences in experimental and analytical load-deformation response of these membranes could be attributed to residual stresses from restrained shrinkage.

Results from the analytical model for the tension stiffening effect while excluding and including the effect of restrained shrinkage, is plotted in Fig. 4 for normal strength reinforced concrete membranes. In Fig. 4, a typical experimental response is also included for comparison purpose.

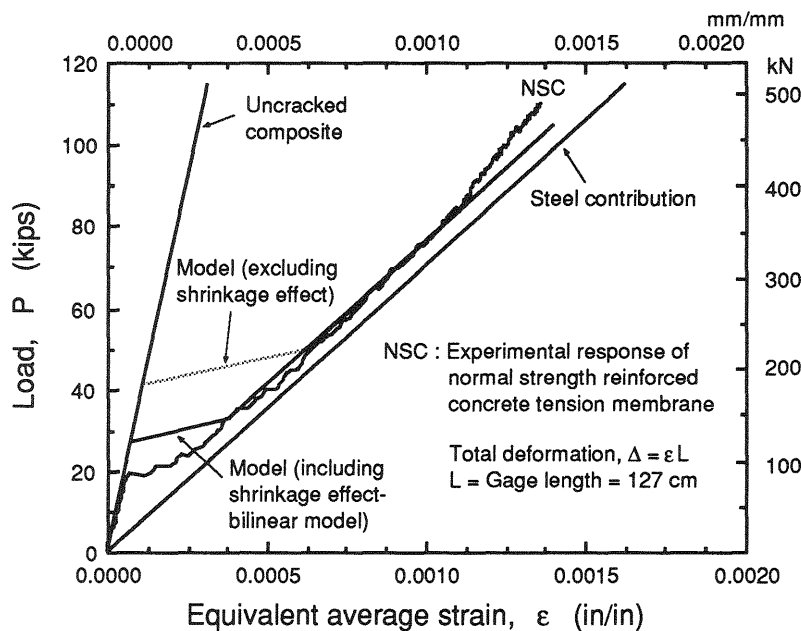


Fig. 4. Load-average strain response for normal strength reinforced concrete tension member showing differences in response due to restrained shrinkage effect

It is convenient to plot the total deformation of the reinforced membrane specimens as equivalent average strain so that comparisons to strains values that characterize the constituent material behavior (concrete cracking, steel yielding) can be readily made. Fig. 4 include bounds for composite load-average strain behavior which are indicated as "uncracked composite" and "steel contribution". The stiffness of the uncracked composite is obtained from the law of mixtures assuming iso-strain behavior. Steel contribution is established based on results from the tension test on the reinforcing steel and steel content. A three-stage analytical model is used to represent the tensile response of a reinforced concrete membrane. Stage I represents elastic behavior of the composite prior to transverse cracking. Stage III, where no new cracks form, and where increased deformations result in increased crack-widths, represents the steady-state crack configuration. Sandwiched between these two stages is Stage II which is the multiple cracking stage.

The influence of restrained shrinkage is most predominant prior to the formation of the first transverse crack and decreases as the number of transverse cracks increase. This is because cracking results in a redistribution of stresses. Additionally, at the larger displacements, the contribution of concrete to the total load-carrying capacity itself also decreases. During the stage of steady-state crack extension (Stage III), restrained shrinkage stresses have negligible influence on the overall load-average strain response of reinforced concrete tension membranes. Fig. 4 accordingly shows the effect of incorporating the effect of restrained shrinkage during Stage II of the load-average strain response. The tensile stiffening model response that does not include the effect of restrained shrinkage is shown using a dotted line, while a solid black line is used to show the response that includes this effect.

As observed from Fig. 4, the simple tri-linear analytical model appears to capture the overall nature of the load-average strain response quite well. Model predictions are generally good for all stages of loading for reinforced concrete specimens.

Although the tension capacity of concrete is typically ignored in the design of reinforced concrete structural components, cracking and related stiffness degradation is important in several secondary design considerations such as limiting deflections and crack widths. From a practical standpoint it would be necessary to be able to predict the cracking load accurately since significant degradation of stiffness takes place soon after first-crack (Fig. 4), even if the post-cracking stiffness is of less importance.

5 Conclusions

- The simple one-dimensional model used to obtain the maximum residual stress due to restrained shrinkage in steel and concrete constituents of a reinforced concrete member predicts experimentally measured shrinkage strains reasonably well.
- The maximum tensile residual stress in concrete predicted using the bilinear model (conservative estimation of residual stress) of approximately 40% of the tensile strength highlights the importance of incorporating the effect of restrained shrinkage to predict first crack loads and moments in structures undergoing drying.

- In addition to a loss of the tensile strength capacity, the loss in strain capacity and associated residual energy stored are expected to influence brittle fracture analysis of concrete.
- Since the drying process is size and geometry dependent, residual stress due to restrained shrinkage contributes to size and geometry dependence of reinforced specimens undergoing drying. If size or geometry effects of brittle fracture are being studied one cannot ignore effects due to restrained shrinkage. However, residual stress due to restrained shrinkage does not significantly impact conventional design of reinforced concrete elements where tension capacity of concrete is typically ignored.

5 References

ACI Committee 209 (1992) Prediction of Creep, Shrinkage and Temperature Effects in Concrete Structure (209R-82). **ACI Manual of Concrete Practice Part 1**.

Ahn, T.S. (1995) **Tension Stiffening in Reinforced Concrete Membranes**. Ph.D. Dissertation, University of Missouri-Columbia.

Bazant, Z.P. (1982) Mathematical Models for Creep and Shrinkage of Concrete, in **Creep and Shrinkage in Concrete Structures** (eds Z.P. Bazant and F.H. Wittmann), John Wiley and Sons, 163-256.

Wittmann, F.H. (1982) Creep and Shrinkage Mechanisms, in **Creep and Shrinkage in Concrete Structures** (eds Z.P. Bazant and F.H. Wittmann), John Wiley and Sons, 129-161.